Proceedings Paper:

Colombo, M and Fairweather, M (2017) CFD Simulation of Boiling Flows with an Eulerian-Eulerian Two-Fluid Model. In: Proceedings of the 17th International Topical Meeting on Nuclear Reactor Thermal Hydraulics. 17th International Topical Meeting on Nuclear Reactor Thermal Hydraulics (NURETH-17), 03-08 Sep 2017 .

CFD SIMULATION OF BOILING FLOWS WITH AN EULERIAN-EULERIAN TWO-FLUID MODEL

Marco Colombo and Michael Fairweather
School of Chemical and Process Engineering, University of Leeds, Leeds LS2 9JT, United Kingdom
M.Colombo@leeds.ac.uk; M.Fairweather@leeds.ac.uk

ABSTRACT
In the nuclear field, computational fluid dynamics (CFD) is being applied increasingly often to improve the prediction of the boiling flows that are to some extent experienced in almost all water-cooled reactors. For reactor-scale flows, although the development of advanced CFD methods is progressing at a fast rate, Eulerian-Eulerian averaged two-fluid models still represent the only practicable option. In these models, boiling at the wall is normally incorporated using the heat flux partitioning approach and, overall, a number of sub-models and closure relations are required, some of which still rely mainly upon empirical arguments. In view of this, further progress is needed in our ability to model and predict boiling flows and, eventually, extend the modelling to other areas such as the prediction of the critical heat flux.
The present paper discusses the development of an Eulerian-Eulerian two-fluid model, implemented in the STAR-CCM+ CFD code. The model includes a Reynolds stress multiphase turbulence model and the S_γ population balance model with improved breakup and coalescence sources. Turbulence and average bubble diameter predictions are firstly, and independently, validated against air-water bubbly flows. Finally, the whole boiling model is assessed against a large database of subcooled boiling flows that covers an extended range of flow conditions. Validation is extended to some recent experiments and some sensitivity studies are made on the modelling of interfacial forces and condensation in the bulk of the flow. Overall, many areas of the model reach a satisfactory accuracy, but a number of weaknesses still persists and, consequently, areas of further improvement are identified.

KEYWORDS
Computational fluid dynamics, two-fluid model, bubbly flow, subcooled boiling

1. INTRODUCTION

During boiling, heat transfer is very efficient and significant amounts of heat can be transferred with minimum temperature differences. Therefore, boiling flows are common in many engineering processes and rather popular in the nuclear reactor industry. Boiling, this being subcooled or saturated, normally occurs in water-cooled reactors, in systems or loops operating in natural circulation that are designed to operate in the boiling regime and, during design-based or beyond-design based accidents, boiling may occur due the decrease in pressure or the reduced coolant inventory. Additionally, high heat transfer rates are guaranteed only as long as the critical heat flux (CHF) is not exceeded. Beyond this limit, the heat transfer deteriorates rapidly, making the CHF perhaps the major threat to the integrity of the fuel rods. Therefore, confident and accurate predictions of boiling and the CHF, and a reduction of the empiricism in modelling, would be of immense benefit to reduce excessive conservatism and increase the safety and efficiency of modern reactors.

Unfortunately, robust and reliable modelling of boiling is not yet available and numerical tools are still based mainly on empiricism, and a long journey is yet in front of us before we will be able to model and predict with accuracy the physics of boiling at the smallest scales [1]. Over the years, progressively more advanced numerical tools have been developed and, most recently, computational fluid dynamic (CFD) approaches have attracted a great deal of attention. Ultimately, with respect to most of the predictive methods currently used in the nuclear industry, CFD can achieve a greater level of detail and potentially describe with accuracy phenomena across the different length scales encountered. Recent advances in direct numerical simulation techniques have also improved our level of knowledge of bubbly and boiling flows and can be expected to continue to corroborate experimental evidence in support to model development [2-4].

Obviously, the level of detail comes at the expense of computational time and, between CFD approaches, Eulerian-Eulerian averaged two-fluid models are at the present time the only realistic option to handle industrial-scale multiphase engineering calculations. In the majority of cases, some boiling capabilities have been incorporated in these models following the Rensselaer Polytechnic Institute (RPI) heat flux partitioning approach [5]. In the RPI model, the heat flux from the wall is partitioned between the mechanisms responsible for heat transfer, identified as single-phase convection, quenching and evaporation. Even if built on a mechanistic approach, RPI-based models are still forced to rely on a number of empirical or semi-empirical closure relations [6]. Most often, a limited general applicability has been achieved and calibration of models on a case-by-case basis has been necessary to obtain a good accuracy, even against a limited number of experiments [7-9].

The complexity of boiling flows extends well beyond the boiling model itself. These are normally polydispersed flows in which the bubble size distribution evolves continuously and bubbles, after detachment from the wall, experience evaporation/condensation and breakup and coalescence. Breakup and coalescence in the bulk of the flow are strongly and mutually coupled to the continuous phase turbulence and velocity fields. Turbulence models have been mainly based on extension to multiphase conditions of two-equation single-phase turbulence models based on an eddy viscosity approach, with Reynolds stress formulations having received more limited attention [10, 11]. In two-fluid models, knowledge of the average bubble diameter is essential because all the interphase transfer processes are proportional to the available interfacial area density. Tracking of the bubble diameter distribution has been often achieved by coupling the two-fluid model with population balance approaches [9, 12, 13]. The approaches available include the volumetric interfacial area concentration equation [12], multiple bubble size group models [9] and models based on the moments of the bubble size distribution [13]. In these, bubble breakup and coalescence are accounted for with numerous formulations, although none of the various approaches has been clearly demonstrated to have a superior performance [14, 15].

In this work, research activities that are still ongoing at the University of Leeds for the development of an advanced Eulerian-Eulerian CFD two-fluid boiling model, solved with the STAR-CCM+ CFD code [16], are presented. In the paper, an overview is given of the entire basis and validation of the model, which was necessarily achieved step-by-step because of the complex and mutual non-linear interactions between the different physical processes. The model includes a multiphase Reynolds stress turbulence formulation that considers a bubble-induced turbulence contribution and the S_γ population balance model, based on the moments of the bubble size distribution. The turbulence model and the S_γ model, which includes improved models of breakup and coalescence, were independently validated against air-water bubbly flows, and the validation is here extended to some recent pipe flow measurements. The complete CFD model, obtained by adding a wall boiling model based on the RPI approach, is assessed against a database of subcooled boiling flows in vertical pipes and annular channels. Some additional sensitivity studies are made in regards to the condensation in the bulk and the role of interphase forces, and areas of further improvement are identified. Overall, almost 50 different flows were used over the entire validation process and the necessity to validate these models, and any new improvements, over large databases that include extended ranges of flow conditions, rather than on a case-by-case basis, is emphasized. This is particularly important for the confident application of CFD models to nuclear reactor thermal hydraulics.

2. THE MODEL

In the two-fluid model, averaged continuity, momentum and energy conservation equations are solved for each phase [17]. Because of averaging, closure models are required for mass, momentum and energy transfers at the interphase. In the momentum equation, drag and turbulent dispersion are modelled following Tomiyama et al. [18] and Burns et al. [19], respectively. Constant lift coefficients are used and the Antal et al. [20] model for the wall force, with more details on the specific values of the coefficients given in [11]. In boiling flows, the role of lift and wall forces is much less well-understood and both forces have been neglected. Turbulence is solved in the continuous phase only with a multiphase extension of the quadratic Reynolds stress model (RSM) proposed by Speziale et al. [21]. In the dispersed phase, turbulence is related to the continuous phase turbulence using a response model. The contribution of bubbles to the continuous phase turbulence is accounted for using a bubble-induced turbulence model, based on the mixed bubble-induced time scale τ_{BI} proposed in [22] and optimized in [11]. The model assumes that the energy lost to drag is converted into turbulence kinetic energy in the bubble wakes and sources of turbulence kinetic energy k and turbulence dissipation rate ε as specified, respectively, as:

$$S_k^{BI} = C_{k,BI}\boldsymbol{F_d}\boldsymbol{U_r} \qquad S_{\boldsymbol{\varepsilon}}^{BI} = \frac{C_{\varepsilon,BI}}{\tau_{BI}}S_k^{BI} = C_{\varepsilon,BI}\frac{k^{0.5}}{d_B}S_k^{BI} \tag{1}$$

Here, $\boldsymbol{F_d}$ is the drag force, $\boldsymbol{U_r}$ the relative velocity between the phases and d_B the average bubble diameter, and $C_{k,BI} = 0.25$ and $C_{\varepsilon,BI} = 1.0$. In the RSM, the turbulence kinetic energy contribution is partitioned between the normal turbulent stresses [11]. The bubble diameter distribution, $P(d_B)$, which is assumed to obey a pre-defined log-normal shape, is predicted by means of the S_γ model [13] that solves additional transport equations for the moments of the bubble size distribution density S_γ:

$$S_\gamma = nM_\gamma = n\int_0^\infty d_B^\gamma P(d_B)\, d(d_B) \tag{2}$$

In each transport equation, source terms account for bubble breakup, coalescence, and nucleation and evaporation [16]. Average bubble diameters are derived from the moment densities, which are related to specific flow quantities (S_0 to the bubble number density n, S_2 to the interfacial area concentration and S_3 to the void fraction α). The probability distribution is known by solving two additional transport equations for S_0 and S_2 and, as S_3 is available from the void fraction, the Sauter-mean diameter (SMD), $d_{SM} = S_3 / S_2$, is used to define the average bubble diameter. Breakup and coalescence are assumed to be due to turbulence only and, starting from the work of Yao and Morel [23], sources were adapted for the S_γ approach and implemented inside the code. Breakup and coalescence are evaluated from the frequency of collision (bubble/turbulent eddy for breakup and bubble/bubble for coalescence), breakup/coalescence efficiency and increases in S_γ due to breakup/coalescence events. For both, complete integrals without simplification are numerically solved:

$$\begin{gathered} S_{br} = 0.84\int_0^\infty \frac{\varepsilon^{1/3}(1-\alpha)}{d_B^{2/3}} n d_B^\gamma \\ \left(N_f^{\frac{3-\gamma}{3}} - 1\right)\frac{1}{1+0.42(1-\alpha)\sqrt{We/We_{crit}}} \quad exp\left(-{}^{We_{crit}}/_{We}\right)P(d_B)d(d_B) \end{gathered} \tag{3}$$

$$\begin{gathered} S_{cl} = 0.14\int_0^\infty\int_0^\infty \varepsilon^{1/3} n^2 (d_1+d_2)^2\left(d_1^{2/3}+d_2^{2/3}\right)^{1/2}\left[(d_1^3+d_2^3)^{\gamma/3}\right. \\ \left. -(d_1^\gamma+d_2^\gamma)\right]\frac{1}{g(\alpha)+1.922\alpha\sqrt{We/We_{crit}}} exp\left(-1.02\sqrt{\frac{We}{We_{crit}}}\right)P(d_1)P(d_2)d(d_1)d(d_2) \end{gathered} \tag{4}$$

where $g(\alpha)$ accounts for bubble packing that limits bubble displacement by turbulence [23], N_f is the number of daughter bubbles for each breakup event, fixed at 2, and We is the Weber number. The critical Weber number We_{crit} was assumed equal to 1.24 in both Eqs. (3) and (4) [23].

The heat flux from the wall, following the RPI approach, is partitioned between convection to the single-phase liquid, evaporation and quenching:

$$q_w = \left(q_c + q_q + q_{ev}\right) \tag{5}$$

The quenching heat flux q_q, which accounts for the additional mixing promoted by bubble detachment, is evaluated from Del Valle and Kenning [24] and the evaporative heat flux q_{ev} is:

$$q_{ev} = Nf\left(\frac{\pi d_w^3}{6}\right)\rho_v h_{lv} \tag{6}$$

In the previous equation, the active nucleation site density N, representing the number of nucleation sites per unit area, is calculated from Hibiki and Ishii [25], and the bubble departure frequency f from Cole [26]. To predict the entire database of subcooled boiling flows, two different correlations, from Tolubinsky and Kostanchuck [27], and Kocamustafaogullari [28], were used for the bubble departure diameter d_w and more details are provided in the result section. Usually, evaporation/condensation in the bulk has been evaluated using the Ranz and Marshall [29] correlation to predict the interphase heat transfer coefficient. In this paper, the more recent correlation from Kim and Park [30] is also tested:

$$Nu = 0.2575 Re_b^{0.7} Pr_l^{-4564} Ja^{-0.2043} \tag{7}$$

where Re_b is the bubble Reynolds number, Pr_l the Prandtl number of the liquid phase and Ja the Jakob number. The overall model, implemented in the STAR-CCM+ CFD code [16], was solved in a two-dimensional axisymmetric geometry. At the inlet, fully-developed single-phase liquid velocity, turbulence and temperature were imposed, together with an imposed pressure at outlet and the no-slip condition, and an imposed heat flux, at the wall. Constant thermophysical properties were imposed. For boiling flows, these were calculated at the average temperature between the inlet and saturation values, for the liquid phase, and at the saturation temperature for the vapour phase. A mesh sensitivity study demonstrated that mesh-independent solutions were achieved with an equidistant structured mesh with the first grid point located at $y^+ > 30$, high enough to apply the high-Reynolds wall treatment.

3. EXPERIMENTAL DATA

A total of 29 pipe air-water bubbly flows and 20 subcooled boiling flows in pipes and annular channels were used during the validation process. Data were taken from [31-36] for the turbulence model validation and from [37-40] for the population balance model validation. Details on the specific experiments can be found in [11] and [41]. In addition, some data were added from the recent CHAPTAL experiment (Table I) for bubbles of refrigerant R116 in water [42]. These data are particularly valuable because they provide measurements of all the physical variables, including turbulence velocities, at different axial locations. The subcooled boiling flow database includes pipe flow experiments from Bartolomei and Chanturiya [43] and Bartolomei et al. [44] for water and from the DEBORA experiment [45] for refrigerant R12, and the annular channel flow experiments of Lee et al. [46] for water and Roy et al. [47] for refrigerant R113. More details of the specific conditions can be found in [48].

Table I. Experiments from the CHAPTAL database used in the validation

Experiment	Γ_w [kg/s]	Γ_g [kg/s]
1	2.272	0.028
2	2.725	0.028
3	1.132	0.014

4. RESULTS AND DISCUSSION

For reasons of space it was not possible to report the entire validation. For clarity, the specific experiments presented in the various plots are summarized in Table II. A first set of pipe flow simulations was made to validate the turbulence model. In these, constant values of the bubble diameter were used, taken equal to average values from experiments. An example is reported in Figure 1 and the complete set of results can be found in [11]. Turbulence levels were well-predicted using the optimized model in Eq. (1) and comparison with streamwise r.m.s. of the velocity fluctuations from experiments is shown in Figure 1(a) for two different flows. In this, and similarly in all the following plots, symbols are used for experimental data and lines for CFD predictions. On the abscissa, the normalized radius is reported and $r/R = 0$ identifies the pipe centre and $r/R = 1$ the wall. Bubble-induced turbulence was found to contribute a significant portion of the total turbulence intensity. The turbulence structure is anisotropic and the anisotropy was also well-predicted by the RSM (Figure 1(b)). The effect of the turbulence structure on the bubble distribution has not been investigated extensively in the past. The majority of works were focused on pipe flows, where the bubble distribution can be well-predicted by a balance of lift and wall forces, which have been extensively optimized in the past to predict pipe flows in particular. Some recent findings [4, 49], however, seem to support a different role of these forces and further studies on the role of turbulence, which will require a precise knowledge of the turbulence structure, would be beneficial.

Table II. Summary of the experiments presented in the result section

Experiment	Source	j_w [m/s]		j_a [m/s]	
L1	Liu [34]	1.0		0.22	
S1	Serizawa et al. [31]	1.03		0.291	
HT1	Hosokawa and Tomiayama [36]	1.0		0.036	
HI1	Hibiki and Ishii [38]	0.262		0.055	
L2	Liu [37]	1.0		0.2	
H1	Hibiki et al. [39]	0.986		0.242	
H2	Hibiki et al. [39]	2.01		0.471	
Lu1	Lucas et al. [40]	0.255		0.0368	
Experiment	**Source**	**Γ_w [kg/s]**		**Γ_g [kg/s]**	
C1	CHAPTAL [42]	2.272		0.028	
Experiment	**Source**	**p [MPa]**	**G [kg/m^{2}s]**	**q'' [kW/m^2]**	**T_{in} [°C]**
D1	DEBORA [45]	2.62	1996	73.9	68.5
D2	DEBORA [45]	2.62	1985	73.9	70.5
D3	DEBORA [45]	1.46	2023	76.3	39.7
D4	DEBORA [45]	1.46	2028	76.2	34.9
D5	DEBORA [45]	2.62	2981	109.4	69.2
D6	DEBORA [45]	3.01	1007	58.2	64.6
R1	Roy et al. [47]	0.269	565	79.4	42.7
R2	Roy et al. [47]	0.269	785	95.0	50.2
Le1	Lee et al. [46]	0.101	714	197.2	86.2
B1	Bartolomei and Chanturiya [43]	1.5	900	380	138.3
B2	Bartolomei et al. [44]	6.89	1500	1200	221.9

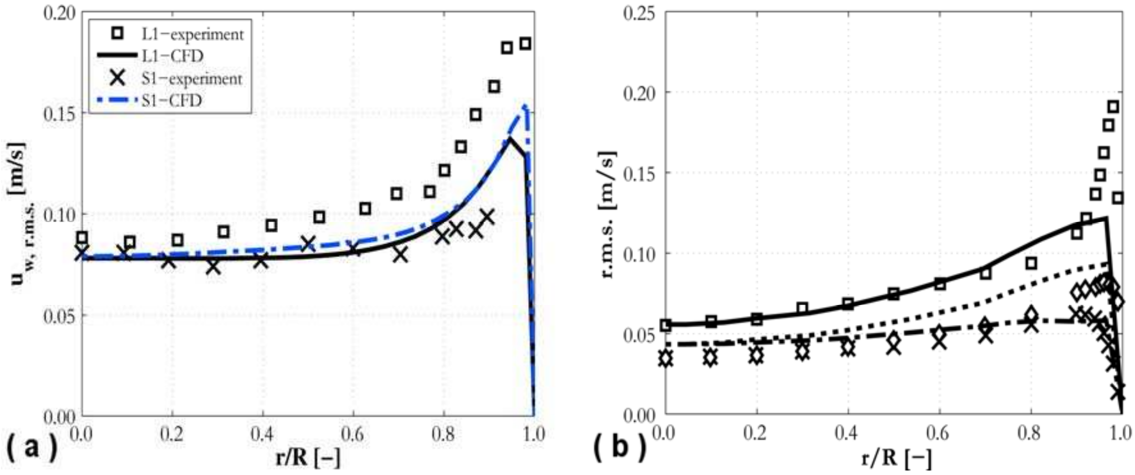

Figure 1. Predicted streamwise r.m.s. (a) and r.m.s. (b) of the turbulent velocity fluctuations compared against experiments. (b): HT1; (□,—) streamwise; (x,– · –) radial; (◊,---) azimuthal.

Figure 2 demonstrates how important good predictions of turbulence are for the accuracy of the population balance model. Predictions of radial profiles of the average bubble diameter (Figure 2(a)) and turbulence intensity (Figure 2(b)) are compared against experiments. Two sets of CFD results are provided, which were obtained with and without considering the bubble-induced turbulence contribution. Since this was proven to be significant in these bubbly pipe flows, the predicted turbulence intensities differ significantly in Figure 2(b). Consequently, and since turbulence is a major contributor to breakup and coalescence, the predicted average bubble diameters differ significantly and are markedly overestimated because of the excessive coalescence at low turbulence levels. In view of this, any validation of the average bubble diameter predictions requires confidence in the accuracy of the coupled turbulence model. Unfortunately, turbulence and bubble diameter measurements are rarely available for the same experiment, and turbulence was measured in only one of the flows presented in Figure 2.

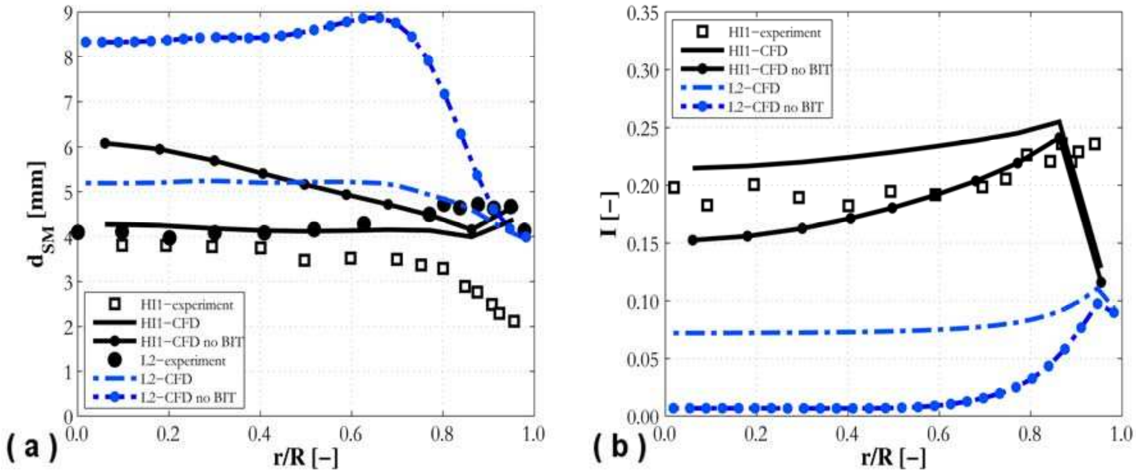

Figure 2. Predicted radial profiles of SMD (a) and turbulence intensity (b) compared against experiments. BIT = bubble-induced turbulence.

More results from the S_γ model are shown in Figure 3. Radial profiles of liquid velocity and void fraction are provided in Figure 3(a) and 3(b), respectively. These are well-predicted for both wall-peaked and higher-void core-peaked void profiles and a similar accuracy was also found for the flows used in the turbulence model validation, although results are not shown. Predictions of the average bubble diameter are shown in Figure 3(c) for two flows. Overall, the accuracy is generally satisfactory, even though there is a tendency for the model to predict excessive coalescence in low-velocity flows, where coalescence is dominant, and excessive breakup in high-velocity flows, where instead breakup is dominant. Therefore, both phenomena seem to be overpredicted, and breakup particularly near the wall where turbulence levels are higher.

Additional validation against the CHAPTAL experiment [42] is presented in Figure 3(d). Recently published, this database contains measurements at increasing axial length and is one of the few cases where velocity, void fraction, bubble diameter and turbulence levels were measured in the same experiment. Inlet conditions were imposed from measurements at the first axial location. The reasonable accuracy of the model is confirmed, and also the tendency to predict excessive coalescence and breakup. In the centre of the pipe, where coalescence is higher, bubble diameter is rather well-predicted, although overestimated. In contrast, near the wall, where breakup is dominant, the bubble diameter is underpredicted.

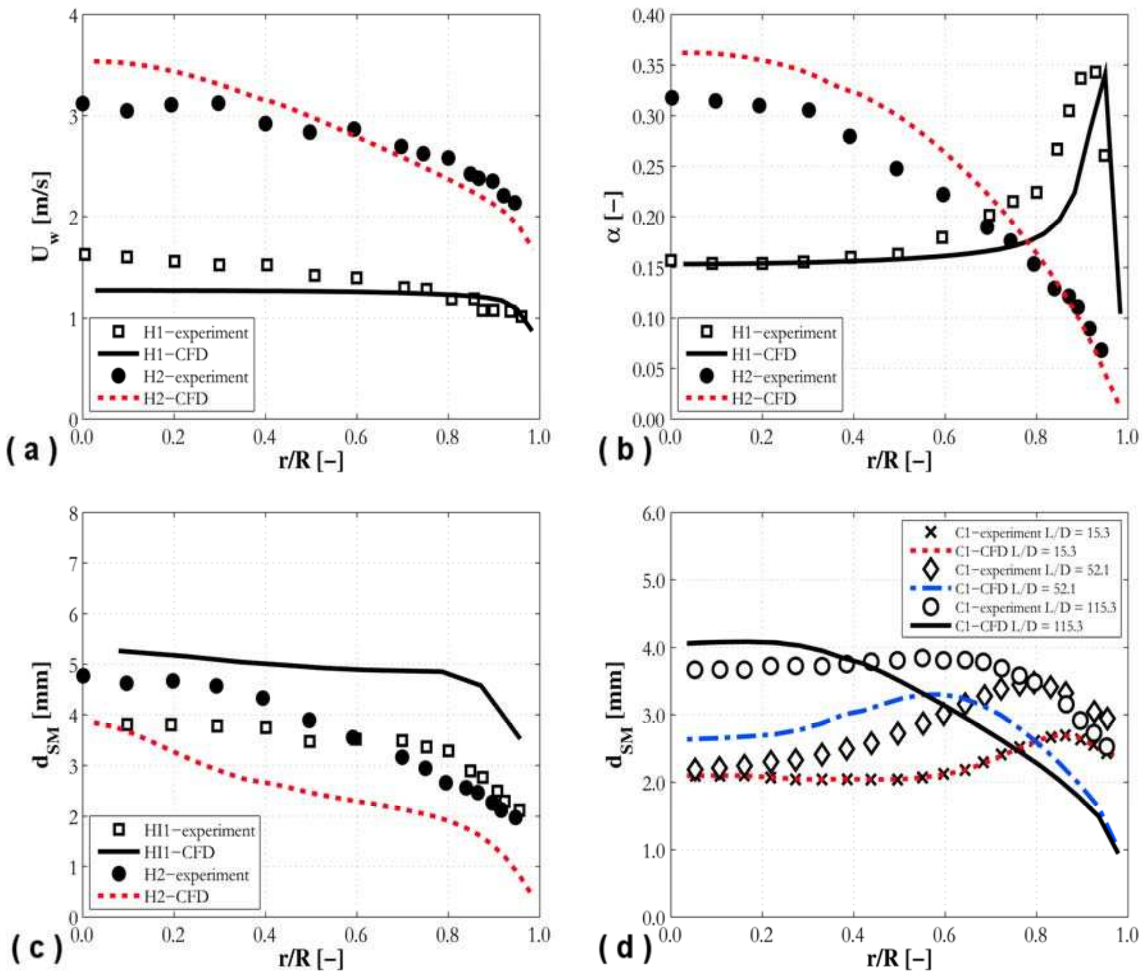

Figure 3. Predicted radial profiles of liquid velocity (a), void fraction (b) and SMD (c-d) compared against experiments.

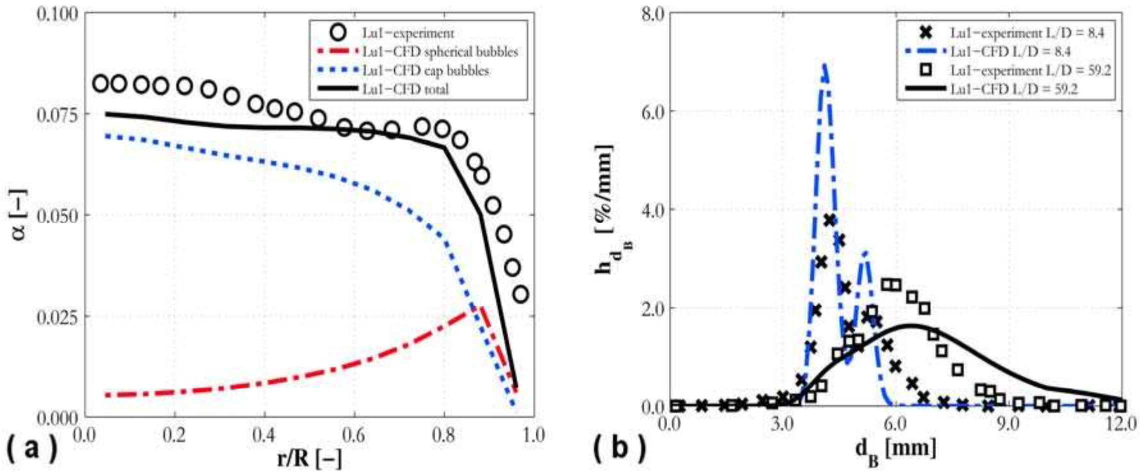

Figure 4. Predicted radial void fraction profile (a) and bubble diameter distribution (b) compared against experiment Lu1.

An extension of the previous model is presented in Figure 4. In this bubbles are divided between smaller, spherical bubbles that move towards the wall and larger, cap bubbles which tends to flow to the centre of the pipe. A separate set of conservation and population balance equations, including the additional exchange terms, were solved for each of the two groups. The model predicts well the void profiles of both groups, and the total void fraction, with spherical bubbles peaking at the wall and cap bubbles in the centre (Figure 4(a)). Therefore, with this model, mixed void profiles, which show features of both groups that make them particularly difficult to reproduce, can be predicted. Bubbles, which are injected at an almost constant diameter, develop a distribution that, due to coalescence, immediately starts to show a second peak at a higher diameter (Figure 4(b)). Progressively, larger bubbles are formed and the distribution is therefore shifted to higher diameters. This trend is well-captured by the model, which seems able to reproduce the behaviour of bubbles in the whole bubbly flow regime, up to the transition to slug or plug flow.

The subcooled boiling database was finally predicted by coupling the turbulence and S_Y models to boiling at the wall. An overview of the results is provided in Figure 5, where vapour velocity, turbulence, void fraction, SMD and liquid temperature radial profiles, and area-averaged void axial profiles, are presented for a number of flows from the database. Since both pipe and channel flows are included, r^* on the abscissa generally refers to a normalized radial distance in Figure 5. More specifically, the heated wall is located at $r^* = 0$ (the inner wall) for annular flows [46, 47], whereas it remains at $r^* = 1$ for pipe flows [43, 44, 45]. In the comparisons, the CFD model parameters fixed for the entire database are maintained to avoid a case-by-case optimization of the parameters.

Overall, agreement is good in many areas and satisfactory predictions were obtained for velocity profiles in pipes (Figure 5(a)) and turbulence levels, with the anisotropy of the turbulence also well-predicted (Figure 5(b)). Good agreement was also found for void fraction and liquid temperature. Therefore, results confirm the potential of CFD to predict boiling flows with accuracy in a wide range of conditions. Unfortunately, not all areas of the flow were well-predicted. Poor accuracy was generally found for the SMD, and also the velocity profiles near the wall in annular channels, although these are not shown in Figure 5. More specifically, average bubble diameter is underestimated in the entire pipe and, in annular channels, velocity was found to peak much closer to the wall with respect to experiments and to be overpredicted in most of the near-wall region.

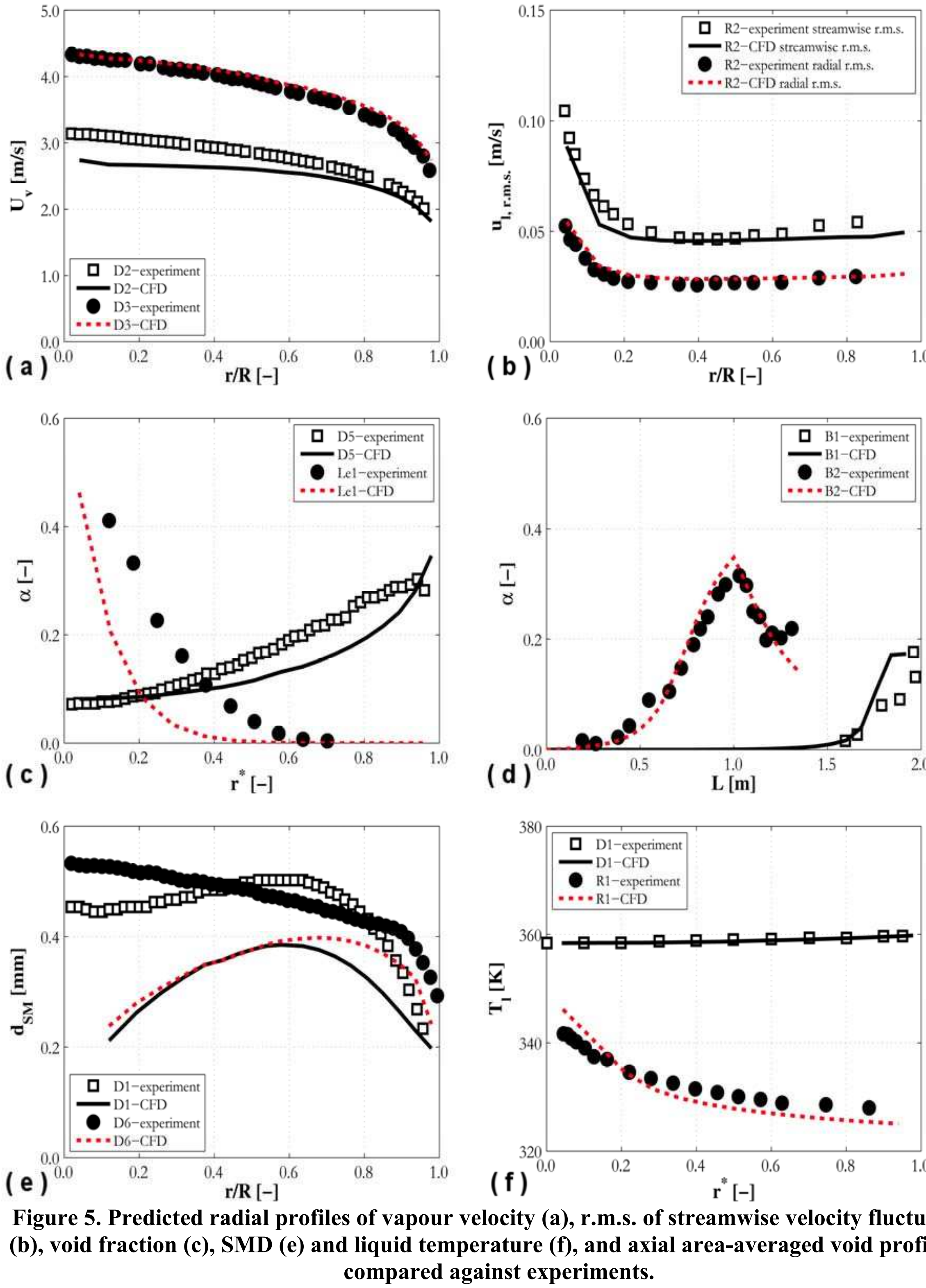

Figure 5. Predicted radial profiles of vapour velocity (a), r.m.s. of streamwise velocity fluctuations (b), void fraction (c), SMD (e) and liquid temperature (f), and axial area-averaged void profiles (d) compared against experiments.

The overestimation of the velocity near the wall is likely related to the wall treatment, which is limited to the single-phase wall function in the present work. It is, however, much more difficult to identify the specific reasons for the underpredicted bubble diameter as different phenomena may contribute. The accuracy of the bubble breakup and coalescence models is a concern, as well as the inability of the overall model to correctly account for larger bubbles, less subjected to subcooling, that can be expected to flow in the higher subcooling region near the centre of the pipe. The other area of uncertainty is the boiling model and more specifically the many empirical relations necessary to close the evaporative heat flux model, which clearly limits the general applicability of the CFD model. Even if all the other model parameters were kept constant, it was not possible to use the same bubble departure correlation over the entire database, with both the models from Tolubinsky and Kostanchuck [27] and Kocamustafaogullari [28] having been used. These are known to have a limited accuracy when used over extended ranges of parameters [50].

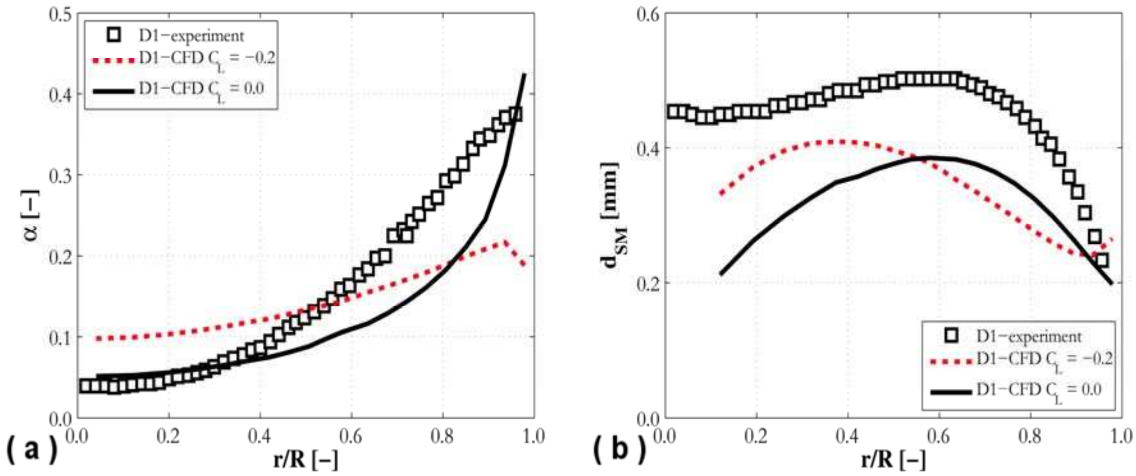

Figure 6. Predicted radial profiles of void fraction (a) and SMD (b) for different values of the lift coefficient C_L compared against experimental data.

In view of the less satisfactory prediction of the average bubble diameter, additional sensitivity studies were made on some of the parameters within the CFD model. Lift and wall forces were neglected in the boiling simulations. Since underestimation of the bubble diameter was observed, particularly near the centre of the pipe (Figure 5(e)), some flows were simulated with a negative lift, this being used to promote migration of the bubbles towards that region of the pipe. Results are again shown in Figure 6. Void fraction prediction is worsened (Figure 6(a)) and only a slight improvement is observed in the SMD radial profile. In other flows, void fraction was improved and almost negligible changes in the bubble diameter profile were sometimes observed. Overall, results are not definitive and benefits are difficult to quantify because of the simultaneous influence of many other effects. Also, the role of wall and lift forces in boiling flows is still very uncertain, and optimization of the lift force on a case-by-case basis is not likely to improve the general applicability and physical consistency of the overall model. Therefore, and until better understanding is available, lift and wall forces are neglected in the present boiling model.

Lastly, Figure 7 compares two correlations for the condensation in the bulk of the fluid. The interphase heat transfer coefficient is calculated using the usual Ranz and Marshall [29] correlation and the more recent one proposed by Kim and Park [30]. Using Kim and Park, the SMD profile remains flatter towards the centre of the pipe, even if it is still underpredicted (Figure 7(a)) and, in Figure 7(b), prediction of the area-averaged void fraction is improved. In other flows, results obtained using the two correlations were more similar. Again, precise quantitative evaluation of the improvement observed is complicated by the simultaneous influence of many different physical effects. Nevertheless, the Kim and Park [30] approach has to be preferred in view of the present results and a recent validation against condensation data and other literature correlations [51].

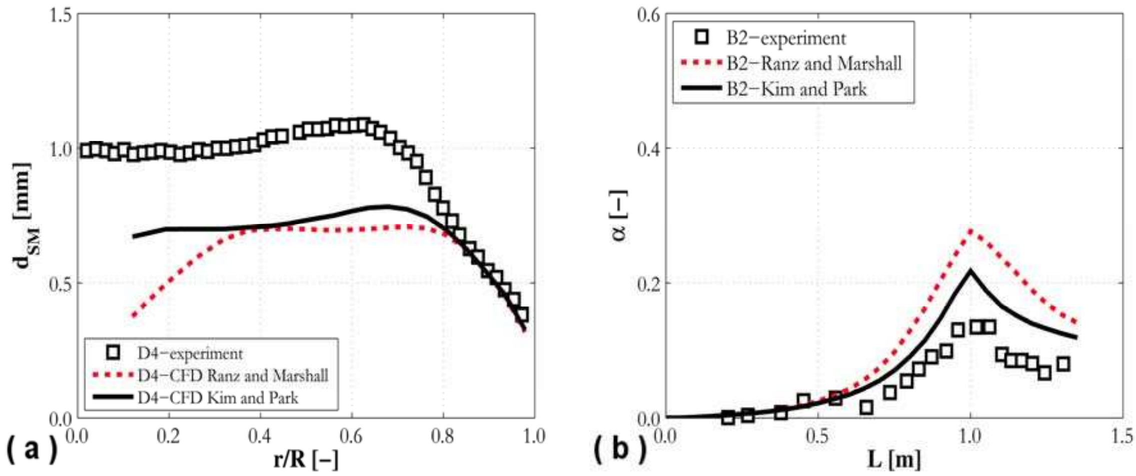

Figure 7. Predicted radial profiles of SMD (a) and axial profiles of area-averaged void fraction (b) using different correlations for the interphase heat transfer coefficient compared against experiments.

5. CONCLUSIONS

With the aim of improving our predictive capabilities for boiling flows, the development of a two-fluid Eulerian-Eulerian CFD model, implemented in the STAR-CCM+ code, was presented in this paper. The focus of the paper was a comprehensive overview of the entire model development and validation process. Because of the complexity of boiling flows and the numerous physical phenomena involved, the model was validated step-by-step by comparing against large databases that include extended ranges of flow conditions. A multiphase RSM model and the S_γ population balance approach with improved models for bubble breakup and coalescence were independently validated against air-water bubbly flows. Accurate predictions of the turbulence field were obtained using the RSM by adding the bubble-induced contribution and accommodating the anisotropy of the turbulence field. Because of the role of turbulence in breakup and coalescence models, accurate turbulence modelling is a prerequisite for any meaningful validation of population balance predictions. The S_γ model shows a satisfactory accuracy, although both breakup and coalescence seem overestimated.

In subcooled boiling flows, the CFD model, where wall boiling is modelled following the RPI approach, achieved a satisfactory accuracy in many areas, such as the velocity, void fraction and temperature fields, confirming the potential of CFD approaches in predicting boiling flows with improved accuracy and levels of detail. Some benefits were obtained using the recent correlation from Kim and Park [30] to evaluate interphase heat transfer and condensation in the bulk. However, poor predictions were obtained in other areas, such as the average bubble diameter and various areas for future model improvement were identified. Overall, the many closures required, often based on a significant amount of empiricism, limit the general applicability of the model. In view of this, substitution of the empirical correlations still used in the wall boiling model with more mechanistic approaches is desirable. In the population balance approach, the breakup and coalescence models can be further improved, and in a similar way the ability to track larger diameter bubbles that flow to the centre of the pipe requires further development. The inability to predict their presence is likely one of the reasons for the underestimation of the bubble departure diameter. Extension to boiling conditions of a two-group model, able to reproduce the entire bubble diameter spectrum in air-water bubbly flows, will be pursued. Also, interphase forces in both the boiling region and the bulk of the flow, and the wall treatment, require additional knowledge and improvement. As an example, the role of lift and wall forces in boiling flows is still uncertain. Therefore, despite been included in the adiabatic air-water flow model, both have been neglected in the boiling model.

Finally, very large databases were considered and case-by-case tuning of the model was avoided. Comparisons of this kind are vital to assess the accuracy and applicability of any CFD model and to validate any new model improvements. At the same time, and because of the many processes involved, a detailed evaluation of the performance of single sub-models is extremely complicated. Therefore, studies such as this need to be coupled with more detailed analyses aimed at improving specific areas of the overall model.

ACKNOWLEDGMENTS

The authors gratefully acknowledge the financial support of the EPSRC under grant EP/K007777/1, Thermal Hydraulics for Boiling and Passive Systems, part of the UK-India Civil Nuclear Collaboration.

REFERENCES

1. G. Yadigaroglu, “CMFD and the critical-heat-flux grand challenge in nuclear thermal-hydraulics”, *International Journal of Multiphase Flow*, **67**, pp. 3-12 (2014).
2. G. Tryggvason and J. Buongiorno, “The role of direct numerical simulations in validation and verification, *CFD for Nuclear Reactor Safety Applications OECD-NEA Workshop*, Bethesda, USA, September 14-16, 2010.
3. S. Dabiri and G. Tryggvason, “Heat transfer in turbulent bubbly flow in vertical channels”, *Chemical Engineering Science*, **122**, pp. 106-113 (2015).
4. C. Santarelli and J. Fröhlich, “Direct Numerical Simulation of spherical bubbles in vertical turbulent channel flow. Influence of bubble size and bidispersity”, *International Journal of Multiphase Flow*, **81**, pp. 27-45 (2016).
5. N. Kurul and M.Z. Podowski, “Multidimensional effects in forced convection subcooled boiling”, *9th International Heat Transfer Conference*, Jerusalem, Israel, 1990.
6. R. Thakrar and S.P. Walker, “CFD prediction of subcooled boiling flow with semi-mechanistic bubble departure diameter modelling”, *25th International Conference Nuclear Energy for New Europe* (*NENE 2016*), Portorož, Slovenia, September 5-8, 2016.
7. G.H. Yeoh and J.Y. Tu, “Two-fluid and population balance models for subcooled boiling flow”, *Applied Mathematical Modelling*, **30**, pp. 1370-1391 (2006).
8. B.J. Yun, A. Splawski, S. Lo and C.H. Song, “Prediction of a subcooled boiling flow with advanced two-phase flow models”, *Nuclear Engineering and Design*, **253**, 351-359 (2012).
9. E. Krepper, R. Rzehak, C. Lifante and T. Frank, “CFD for subcooled flow boiling: Coupling wall boiling and population balance models”, *Nuclear Engineering and Design*, **255**, 330-346 (2013).
10. S. Mimouni, J. Lavieville, N. Seiler and P. Ruyer, “Combined evaluation of second order turbulence model and polydispersion model for two-phase boiling flow and application to fuel assembly analysis”, *Nuclear Engineering and Design*, **241**, pp. 4523-4536 (2011).
11. M. Colombo and M. Fairweather, “Multiphase turbulence in bubbly flows: RANS simulations”, *International Journal of Multiphase Flow*, **77**, pp. 222-243 (2015).
12. V.T. Nguyen, C.H. Song, B.U. Bae and D.J. Euh, “Modeling of bubble coalescence and break-up considering turbulent suppression phenomena in bubbly two- phase flow”, *International Journal of Heat and Mass Transfer*, **54**, pp. 31-42 (2013).
13. S. Lo and D. Zhang, “Modelling of break-up and coalescence in bubbly two-phase flows”, *Journal of Computational Multiphase Flow*, **1**, pp. 23-38 (2009).

14. Y. Liao and D. Lucas, "A literature review of theoretical models for drop and bubble breakup in turbulent dispersions", *Chemical Engineering Science*, **64**, pp. 3389-3406 (2009).
15. Y. Liao and D. Lucas, "A literature review on mechanisms and models for the coalescence process of fluid particles" *Chemical Engineering* Science, **65**, pp. 2851–2864 (2010).
16. CD-adapco, *STAR-CCM+® Version 10.04 User Guide* (2015).
17. M. Ishii and T. Hibiki, *Thermo-fluid dynaimcs of two-phase flow*, Springer, New York, USA (2006).
18. A. Tomiyama, I. Kataoka, I. Zun and T. Sakaguchi, "Drag coefficients of single bubbles under normal and micro gravity conditions", *JSME International Journal Series B Fluids and Thermal Engineering*, **41**, pp. 472-479 (1998).
19. A.D. Burns, T. Frank, I. Hamill and J.M. Shi, "The Favre averaged drag model for turbulent dispersion in Eulerian multi-phase flows", *5th International Conference on Multiphase Flow*, Yokohama, Japan, 2004.
20. S.P. Antal, R.T. Lahey Jr and J.E. Flaherty, "Analysis of phase distribution in fully developed laminar bubbly two-phase flow", *International Journal of Multiphase Flow*, **17**, pp. 635-652 (1991).
21. C.G. Speziale, S. Sarkar and T.B. Gatski, "Modelling the pressure-strain correlation of turbulence: an invariant dynamical system approach", *Journal of Fluid* Mechanics, **227**, pp. 245-272 (1991).
22. R. Rzehak and E. Krepper, "CFD modeling of bubble-induced turbulence", *Int. J. Multiphase Flow* **55**, 138-155 (2013).
23. W. Yao and C. Morel, "Volumetric interfacial area prediction in upward bubbly two-phase flow", *International Journal of Heat and Mass* Transfer, **47**, pp. 307-328 (2004).
24. V.H. Del Valle and D.B.R. Kenning, "Subcooled flow boiling at high heat flux", *International Journal of Heat and Mass Transfer*, **28**, pp. 1907-1920 (1985).
25. T. Hibiki and M. Ishii, "Active nucleation site density in boiling systems", *International Journal of Heat and Mass Transfer*, **46**, pp. 2587-2601 (2003).
26. R. Cole, "A photographic study of pool boiling in the region of the critical heat flux", *AIChE Journal*, **6**, pp. 533-538 (1960).
27. V.I. Tolubinsky and D.M. Kostanchuck, "Vapour bubbles growth rate and heat transfer intensity at subcooled water boiling", *4th International Heat Transfer Conference*, Paris, France, 1970.
28. G. Kocamustafaogullari, "Pressure dependence of bubble departure diameter for water", *International Communications in Heat and Mass Transfer*, **10**, pp. 501-509 (1983).
29. W.E. Ranz and W.M. Marshall, "Evaporation from drops", *Chemical Engineering Progress*, **48**, pp. 141-146 (1952).
30. S.J. Kim and G.C. Park, "Interfacial heat transfer of condensing bubble in subcooled boiling flow at low pressure", *International Journal of Heat and Mass Transfer*, **54**, pp. 2962-2974 (2011).
31. A. Serizawa, I. Kataoka, I. Michiyoshi, "Turbulence structure of air-water bubbly flow-II. Local properties", *Int. J. Multiphase Flow* **2**, pp. 235-246 (1975).
32. S.K. Wang, S.J. Lee, O.C. Jones Jr and R.T. Lahey Jr, "3-D turbulence structure and phase distribution measurements in bubbly two-phase flows", *Int. J. Multiphase Flow* **13**, pp. 327-343 (1987).
33. T.J. Liu and S.G. Bankoff, "Structure of air-water bubbly flow in a vertical pipe-I. Liquid mean velocity and turbulence measurements", *Int. J. Heat Mass Tran.* **36**, pp. 1049-1060 (1993).
34. T.J. Liu, "The role of bubble size on liquid phase on liquid phase turbulent structure in two-phase bubbly flows", *Proceedings of the 3rd International Conference on Multiphase Flow*, Lyon, France (1998).
35. O.N. Kashinsky and V.V. Randin, "Downward bubbly gas-liquid flow in a vertical pipe", *Int. J. Multiphase Flow* **25**, pp. 109-138 (1999).
36. S. Hosokawa and A. Tomiyama, "Multi-fluid simulation of turbulent bubbly pipe flow", *Chem. Eng. Sci.* **64**, pp. 5308-5318 (2009).
37. T.J. Liu, "Bubble size and entrance length effects on void development in a vertical channel", *International Journal of Multiphase Flow*, **19**, pp. 99-113 (1993).

38. T. Hibiki and M. Ishii, “Experimental study on interfacial area transport in bubbly two-phase flows”, *International Journal of Heat and Mass Transfer*, **42**, pp. 3019-3035 (1999).
39. T. Hibiki, M. Ishii and Z. Xiao, “Axial interfacial area transport of vertical bubbly flows”, *International Journal of Heat and Mass* Transfer, **44**, pp. 1869-1888 (2001).
40. D. Lucas, E. Krepper and H.M. Prasser, “Development of co-current air–water flow in a vertical pipe”, *International Journal of Multiphase* Flow, **31**, pp. 1304-1328 (2005).
41. M. Colombo and M. Fairweather, “RANS simulation of bubble coalescence and break-up in bubbly two-phase flows”, *Chemical Engineering Science*, **146**, pp. 207-225 (2016).
42. S. Mimouni, C. Baudry, M. Guingo, M. Hassanaly, J. Lavieville, N. Mechitoua and N. Merigoux, “Combined evaluation of bubble dynamics, polydispersion model and turbulence modelling for adiabatic two-phase flow”, *16th International Topical Meeting on Nuclear Reactor Thermal-Hydraulics* (*NURETH 16*), Chicago, USA, August 30 – September 4, 2015.
43. G.C. Bartolomei and V.M. Chanturiya, “Experimental study of true void fraction when boiling subcooled water in vertical tubes”, *Thermal Engineering*, **14**, pp. 123-128 (1967).
44. G.G. Bartolomej, V.G. Brantov, Y.S. Molochnikov, Y.V. Kharitonov, V.A. Solodkij, G.N. Batashova and V.N. Mikhajlov, “An experimental investigation of the true volumetric vapour content with subcooled boiling tubes”, *Thermal Engineering*, **29**, pp. 20-22 (1982).
45. G. Garnier, E. Manon and G. Cubizolles, “Local measurements on flow boiling of refrigerant 12 in a vertical tube”, *Multiphase Science and Technology*, **13**, 1-111 (2001).
46. T.H. Lee, G.C. Park and D.J. Lee, “Local flow characteristics of subcooled boiling flow of water in a vertical concentric annulus”, *International Journal of Multiphase Flow*, **28**, pp. 1351-1368 (2002).
47. R.P. Roy, V. Velidandla and S.P. Kalra, “Velocity field in turbulent subcooled boiling flow”, *Journal of Heat Transfer*, **119**, pp. 754-766 (1997).
48. M. Colombo and M. Fairweather, “Accuracy of Eulerian-Eulerian, two-fluid CFD boiling models of subcooled boiling flows”, *International Journal of Heat and Mass Transfer*, **103**, pp. 28-44 (2016).
49. M. Ullrich, R, Maduta and S. Jakirlic, “Turbulent bubbly flow in vertical pipe computed by an eddy-resolving Reynolds stress model”, *10th International ERCOFTAC Symposium on Engineering Turbulence Modelling and Measurements*, Marbella, Spain, September 17-19, 2014.
50. R. Thakrar, J.S. Murallidharan and S.P. Walker, “An evaluation of the RPI model for the prediction of the wall heat flux partitioning in subcooled boiling flows”, *22nd International Conference on Nuclear Engineering (ICONE 22)*, Prague, Czech Republic, July 7-11, 2014.
51. G. Rabello dos Anjos and J. Buongiorno, “Bubble condensation heat transfer in subcooled flow boiling at PWR conditions: a critical evaluation of current correlations”, *CASL-U-2013-0199-000*.